# Mode coupling effects in Ring-Core Fibres for Space-Division Multiplexing Systems

X.Q. Jin, A. Gomez, Kai Shi, Benn C. Thomsen, Feng Feng, George S. D. Gordon, Timothy D. Wilkinson, Y. Jung, Q. Kang, P. Barua, J. K. Sahu, S. Alam, D. J. Richardson, D.C. O'Brien, and F.P. Payne

***Abstract*— An optical fibre with weak mode coupling is desirable for future ultra-high capacity space-division multiplexing (SDM) systems because mode coupling in an optical fibre results in extrinsic loss of the fibre and crosstalk between guided optical modes. To study the feasibility of a ring-core fibre (RCF) for SDM systems, in this paper, we investigate the mode coupling in the RCF supporting up to 5 or 7 guided mode groups (MGs) at a wavelength of 1550nm. For this purpose, the coupled mode/power theory (CMT/CPT) with a proposed form of the spatial power spectrum of random perturbations of fibre axis is used to calculate the bend loss/crosstalk of the RCF duo to microbending. It is shown that, based on the identified parameters for the spatial power spectrum in the 5/7-MG RCF, the calculated bend loss/crosstalk of the RCF agrees well with experimental results. In addition, the impact of the gradient parameter $\alpha$ and refractive index contrast $\Delta$ of the RCF on bend loss and crosstalk of the RCF is explored. Simulation results show that the $\Delta$ instead of the $\alpha$ significantly affects bend loss and crosstalk of the RCF. The magnitude improvement in bend loss by increasing the $\Delta$ is dependent on the spatial power spectrum rather than the number of guided mode groups in the RCF.**

***Index Terms*—Crosstalk, coupled mode/power theory, mode coupling, microbending, ring-core fibre, space-division multiplexing.**

## I. Introduction

To satisfy the ever-increasing bandwidth demand of optical networks in the next decades, space-division multiplexing (SDM) has been considered as a promising technique for future ultra-high capacity optical networks, because it can overcome the capacity bottleneck imposed by the nonlinear Shannon limit in the single-mode fibre (SMF) [1-3]. The SDM aims to provide a sustainable long-term solution for upgrading the optical network capacity in a cost-effective/energy-efficient manner. The application of SDM mainly lies on new transmission optical waveguides which affect energy efficiency and cost saving in capital and operating expenditure. A number of experimental demonstrations have been reported for high-speed spatial multiplexed transmission over the optical modes in the few-mode/multimode/multi-core/multi-element/ring-core fibres [4-9].

Ring-core fibres (RCFs) have attracted considerable research interest in recent years because of its advantages [10-11], which include simple coupling between RCFs and single-mode fibres (SMFs), and large effective area for reducing nonlinear effect. A photonic integrated circuit with a circular grating coupler was demonstrated experimentally [10], which shows its great advantage of simple and effective mode conversion. In a RCF, the propagation constant difference between adjacent azimuthal modes significantly increases with increasing azimuthal mode number, which in theory may results in relatively weak (strong) mode coupling between high (low) order azimuthal modes. The multiple-input and multiple-output (MIMO) processing used to mitigate the coupling effects may be avoided for the signals carried on the high order azimuthal modes experiencing weak mode coupling. The digital signal processing (DSP) complexity can thereby be reduced by only using MIMO processing to recover signals carried on the low order azimuthal modes which experience strong mode coupling [12]. In addition, a 6-mode-group ring core multimode erbium doped fiber amplifier (EDFA) was proposed, which is shown to be capable of providing nearly identical gain among the 6 mode groups within the C band using a core/cladding-pumped scheme [13].

Both theoretical and experimental investigations have been undertaken for the design of the RCF and modal characteristics in SDM systems [14-20]. Recently, we have designed and fabricated two RCFs with a large refractive index contrast of ~0.01 supporting 5 or 7 mode groups (MGs) (18 or 26 vector modes) at 1550nm for SDM transmission [19-21, 28]. To ease the mode excitation and extraction, these RCFs were usually designed to support one radial mode and multiple azimuthal modes. Therefore, the modes in mode group *l* normally

Manuscript received October ??, 2015. This work was supported by the U.K. Engineering and Physical Sciences Research Council under grant number EP/J008745/1.

X.Q. Jin, A. Gomez, D.C. O'Brien, and F.P. Payne are with the Department of Engineering Science, University of Oxford, Oxford, OX1 3PJ, U.K. (e-mail: xianqing.jin@eng.ox.ac.uk, ariel.gomezdiaz@eng.ox.ac.uk, dominic.obrien@eng.ox.ac.uk, frank.payne@lincoln.ox.ac.uk).

K. Shi and B.C. Thomsen are with the Department of Electronic and Electrical Engineering, University College London, London, WC1E 7JE, U.K. (e-mail: k.shi@ucl.ac.uk, b.thomsen@ee.ucl.ac.uk).

F. Feng, G.S.D. Gordon, and T.D. Wilkinson are with the Department of Engineering, Electrical Engineering Division, University of Cambridge, Cambridge, CB3 0FA, U.K. (e-mail: ff263@cam.ac.uk, gsdg2@cam.ac.uk, tdw13@cam.ac.uk).

Y. Jung, Q. Kang, P. Barua, J. K. Sahu, S. Alam, D. J. Richardson are with the Optoelectronics Research Centre, University of Southampton, Southampton, SO17 1BJ, U.K. (e-mail: ymj@orc.soton.ac.uk, qk1g11@soton.ac.uk, p.barua@soton.ac.uk, jks3@soton.ac.uk, sua@orc.soton.ac.uk, djr@orc.soton.ac.uk).

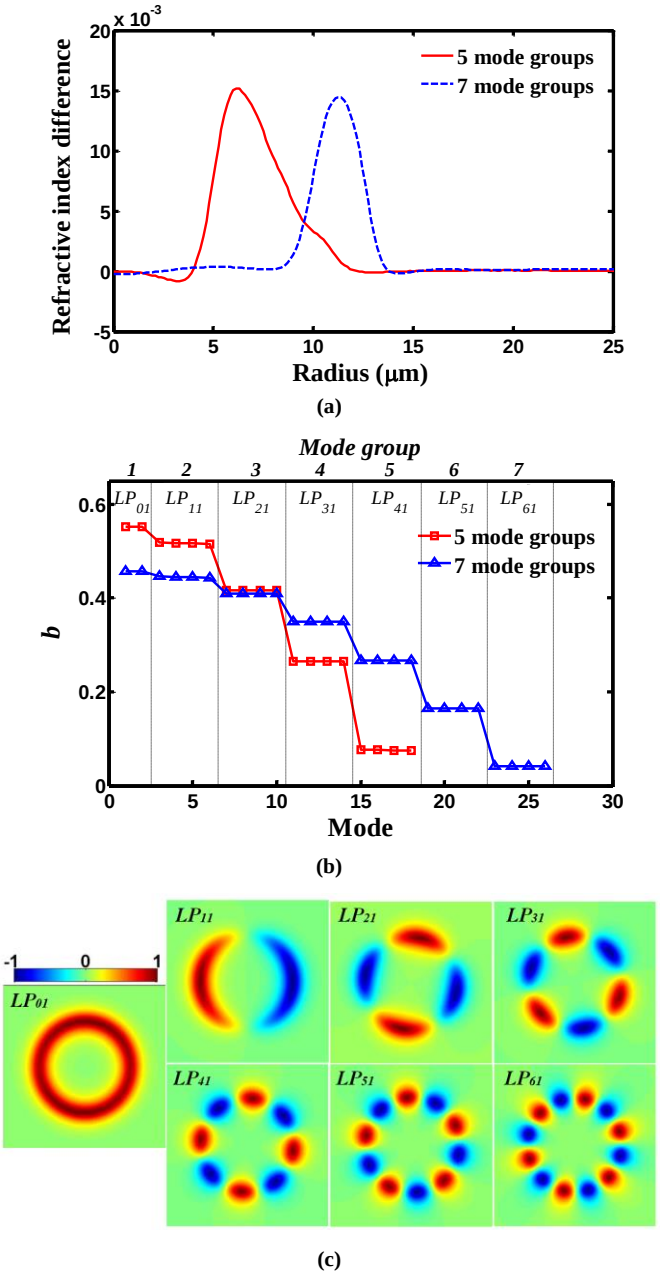


Fig. 1. (a) Refractive index profiles of two fabricated RCFs, (b) its normalized propagation constants *b* of guided vector modes, and (c) Electric fields of LP modes in the 7-MG RCF. Wavelength: 1550nm.

correspond to the linearly polarised (LP) modes, LP($_{l\text{-}1)1}$. When $l \geq 1$, the LP mode has two-fold spatial degeneracy in each polarization. Figs. 1(a-c) show the measured refractive index profiles (RIPs) of these two fabricated RCFs, its normalized propagation constant of vector modes and electric fields of corresponding LP modes, respectively. The experimental characterisation of the RCFs shows that the RCF supporting 7 mode groups suffers a large insertion loss of a few hundred dB/km, whilst the RCF supporting 5 mode groups has a relatively low insertion loss of a few dB/km [20, 21, 28]. It is noted that those fabricated RCFs supporting a large number of spatial modes or mode groups suffer a large insertion loss [16, 18, 20], which restricts their applications for optical communications. Therefore, it is necessary to investigate the cause of such a large insertion loss and impact of key parameters of the RCF design on extrinsic loss of the RCF.

It is well known that microbending plays an important role in the loss of optical fibres because microbending is one of key extrinsic effects increasing attenuation of an optical fibre, apart from the inherent low loss of optical fibres. Microbending occurs in practice when the bending radius is smaller than 1mm, and causes mode coupling between a guided mode and other guided modes or cladding modes, which results in the extrinsic loss of the fibre and crosstalk between optical modes. The extrinsic loss arises from the heavily attenuated power of the cladding modes due to the lossy plastic jacket surrounding the optical fibre. The origin of microbending is usually the lateral contact of the optical fibre with rough surfaces and imperfect optical fibre fabrication processing, which result in high-frequency random perturbations of the fibre core along the fibre axis. Given the difficulty in obtaining characteristics of random perturbations in a practical optical fibre, most research on microbending loss was carried out in theory or simulation. Analytical expressions used to predict microbending loss indicate that the mode coupling between optical modes due to microbending is mainly dependent on the autocorrelation function of the random perturbations and fibre design [22-24].

For a practical RCF, the microbending induced loss and crosstalk may be different from the traditional central core optical fibres, because 1) the special ring-shape RIP of the RCF may result in a special autocorrelation function of the random perturbations of the fibre axis; 2) the RCF has special mode field and normalized propagation constant distributions as seen in Fig. 1. To study the feasibility of a RCF for SDM systems, in this paper, we investigate the microbending induced bend loss and crosstalk in two RCFs supporting 5/7 mode groups, which we recently designed and fabricated [19-21, 28]. With the coupled mode/power theory (CMT/CPT) for the wave propagation analysis [23], the bend loss and crosstalk of the RCF due to microbending are estimated and compared with experimental results. In addition, to improve the bend loss and crosstalk of the RCF, detailed discussions are given to exploration of key parameters of the RCF design affecting SDM applications.

## II. Analytical Expression for Microbending Loss and Impulse Response from Coupled Mode/Power Theory

For an optical fibre with microbends, the distorted refractive index profile $n(r, \varphi, z)$ can be written as a first order Taylor series expression [23].

$$n(r,\varphi,z) = n_0(r) + \frac{\partial n_0}{\partial r} f(z)\cos(\varphi) \qquad (1)$$

where $n_0(r)$ is the undistorted refractive index profile of a perfect fibre, and $r$ is the radial coordinate of a cylindrical coordinate system. $f(z)$ represents random perturbations of the fibre core along the fibre axis. The loss due to microbending is determined by coefficients of mode coupling between a guided mode and discrete cladding modes. The formula for these coefficients includes an integral in the $r$, $\varphi$-plane over the

product $[n(r,\varphi,z)-n_0(r)]E_{lm}E_{l'm'}$. Here, $E_{lm}$ (or $E_{l'm'}$) is the guided (or cladding) mode field, which can be expressed as $A_{lm}(r)\cos(l\varphi)\exp(-j\beta_{lm}z)$ (or $A_{l'm'}(r)\cos(l'\varphi)\exp(-j\beta_{l'm'}z)$). $l$ and $m$ are the azimuthal and radial mode index, respectively. $\beta$ is the mode propagation constant. Since the refractive index difference $(n-n_0)$ contains a term of *cos(φ)*, the coefficients of the mode coupling in the fibre have nonzero values when the azimuthal mode index difference between the guided and cladding modes $|l-l'|$ is one. Therefore, the microbending loss coefficient of a guided mode can be written as [23]

$$2\gamma_{lm}=\sum_{m'=2}^{\infty}\frac{{k_0}^2}{2}\widetilde{R}(\Delta\beta_{lm,l'm'})\frac{\left(\int_0^{\infty}\frac{\partial n_0}{\partial r}A_{lm}A_{l'm'}rdr\right)^2}{\int_0^{\infty}{A_{lm}}^2rdr\int_0^{\infty}\left(A_{l'm'}\right)^2rdr}\qquad |l-l'|=1 \tag{2}$$

where $k_0=2\pi/\lambda$ is the free-space wavenumber ($\lambda$ is wavelength in the free space) and $\Delta\beta_{lm,l'm'}$ is the propagation constant difference between guided and cladding modes. $\widetilde{R}(\Delta\beta)$ is the spatial power spectrum of the autocorrelation function of *f(z)*. To represent a wide range of autocorrelation functions, the spatial power spectrum is given by the form,

$$\widetilde{R}(\Delta\beta)=\frac{C\sigma^2}{1+\left(\Delta\beta L_c\right)^{2p}} \tag{3}$$

$$C=\left[\int_{-\infty}^{\infty}\frac{1}{1+\left(\Delta\beta L_c\right)^{2p}}d\Delta\beta\right]^{-1} \tag{4}$$

where $L_c$ is correlation length and $\sigma$ is the standard deviation of the random perturbation function *f(z)*. A typical value of $p$ is 1, 2, or 3 depending on the external stress on the fibre and fibre fabrication processing.

In order to obtain the impulse response of the RCF-based transmission link for the analysis of crosstalk, mode coupling in the RCF is modelled with the coupled power theory (CPT) or following coupled power equation derived by Marcuse [25].

$$\frac{dP_i}{dz}+\tau_i\frac{dP_i}{dt}=-2\gamma_iP_i+\sum_{i'}\Gamma_{ii'}(P_{i'}-P_i) \tag{5}$$

where $P_i$, $\tau_i$, and $\gamma_i$ are the power, delay per unit length and power attenuation coefficient of guided mode $i$, respectively. Assuming that the inherent low loss of the optical fibre is negligible, the mode power attenuation coefficient can be determined by Eq. (2). $\Gamma_{ii'}$ is the mode coupling coefficient between mode $i$ and $i'$, which can be expressed as [24-25]

$$\Gamma_{ii'}=\widetilde{R}(\Delta\beta_{ii'})\cdot\left|K_{ii'}\right|^2 \tag{6}$$

$$K_{ii'}=\frac{\pi\omega e_0}{2j}\int_0^{\infty}\frac{\partial n_0}{\partial r}A_iA_{i'}rdr \tag{7}$$

The mode coupling coefficient is calculated with the electric field for each mode normalized as follows.

$$\int_0^{\infty}rA_i^2dr=\frac{k_0}{\pi\beta_i}\sqrt{\frac{\mu_0}{e_0}} \tag{8}$$

where $e_0$ and $\mu_0$ are vacuum permittivity and vacuum permeability, respectively. As seen from Eqs. (6-8) that the mode coupling coefficient $\Gamma$ consists of two parts: the spatial power spectrum $\widetilde{R}(\Delta\beta)$ determined by the environment surrounding the fibre and fibre fabrication processing, and the coefficient $K$ determined by the fibre design ($n_0$). In the following, discussion is given to the impact of both the spatial power spectrum $\widetilde{R}(\Delta\beta_{lm})$ and the fibre design on bend loss/crosstalk of the RCF.

## III. Simulation Conditions and Parameters

To study the impact of the fibre design on bend loss/crosstalk of the RCF, the refractive index profile of the RCF is defined as

$$n_0(r)=\begin{cases}n_a\left[1-2\Delta\left(\frac{r-r_a}{d/2}\right)^{\alpha}\right]^{1/2} & |r-r_a|\le d/2\\ n_a\left(1-2\Delta\right)^{1/2} & |r-r_a|>d/2\end{cases} \tag{9}$$

where $n_a$ is the peak refractive index in the ring-core layer, and $\Delta$ is the refractive index contrast. $r_a$ and $d$ are the average radius and thickness of the ring-core layer, respectively. The normalized propagation constant is defined as $b=[(\beta/k_0)^2-{n_c}^2]/({n_a}^2-{n_c}^2)$, where $n_c$ is the cladding index. The measured RIPs in Fig. 1(a) or defined RIP in Eq. (9) are used to obtain the vector mode properties (propagation constants, delay and electric fields) at a wavelength of 1550nm with Comsol. 500 modes including both guided and cladding modes are used for the calculation of the bend loss in Eq. (2).

The crosstalk of the RCF is calculated from the impulse response of the RCF link obtained from Eq. (5). With a split-step method [26], Eq. (5) can be solved numerically when the step $\Delta z$ is smaller than inverse of maximum value of $d_{ij}$. The value of $\Delta z$ is chosen to be $<(20\Gamma_{max})^{-1}$ for high accuracy of channel modelling here, where $\Gamma_{max}$ is maximum value of $\Gamma$. In calculating crosstalk between guided optical modes in the RCF, a mode group carrying a single Gaussian pulse is excited at the input of the RCF to obtain the crosstalk between the launched mode group and other mode groups with the received power in each mode group. The impulse response of the RCF link can also be used to verify the bend loss obtained in Eq. (2). The full-width half-maximum (FWHM) of the Gaussian pulse is 36ps, which corresponds to the 28Gbaud quadrature phase shift keying (QPSK) signal adopted for experimental measurement of crosstalk [28]. An ideal low-pass filter is used to simulate the limited electrical bandwidth of 25GHz for the coherent receiver in the experiment.

## IV. Bend Loss and Crosstalk of the RCF

With the mode coupling theory and model of the optical fibre link described in Section II, investigation is made of comparisons in bend loss/crosstalk between numerical and experimental results. After that, detailed numerical results are given to explore the impact of the fibre design on bend loss and crosstalk of the RCF. As each mode in a mode group suffers equal bend loss due to microbending, for simplicity, guided mode groups instead of vector modes are used for analysis although vector modes or degenerate modes can also be used for mode division multiplexing applications.

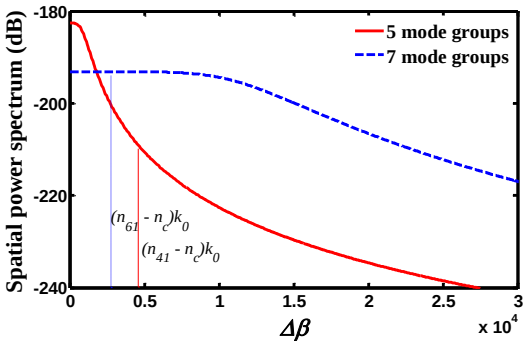


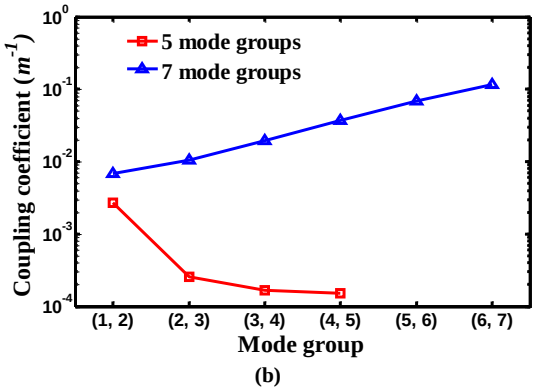


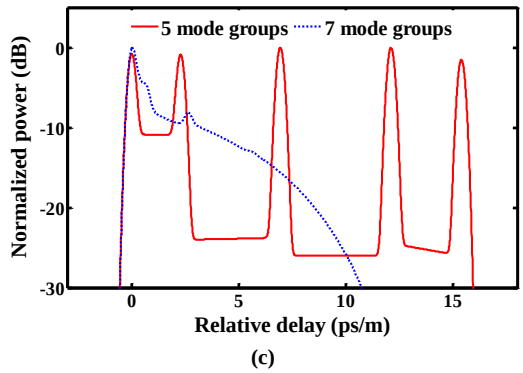


Fig. 2.(a) Spatial power spectrum of the autocorrelation function for the 5/7-MG RCF; (b) Coupling coefficient between two adjacent mode groups, (c) Impulse responses of the 100m 5/7-MG RCFs when all the guided modes are excited at the input with equal power.

### *A. Comparisons between experimental and numerical results*

The mode dependent loss (MDL) was measured by a cutback technique when a guided mode group was selectively launching into the RCFs. To fit the experimental results with numerical results, a proper spatial power spectrum of the autocorrelation function needs to be identified. It can be seen from Eqs. (2-3) that the $\sigma$ determines the average bend loss of the RCF, whilst the correlation length $L_c$ and $p$ determine the slope of the spatial power spectrum or the distribution of the bend loss on all the mode groups. With the above knowledge, a set of parameters, *$\sigma$=35nm (35nm), $L_c$=1mm (0.083mm)* and *p=2 (3)*, were identified for the 5 (7)-MG RCF with the measured RIPs. The graphs of the spatial power spectrum and the coupling coefficient between neighbouring mode groups obtained with the identified parameters are given in Fig. 2(a, b). It shows that

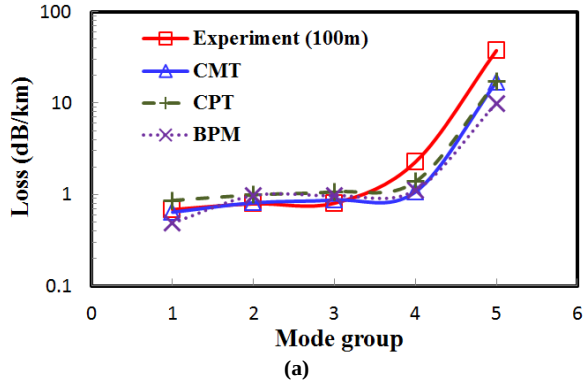


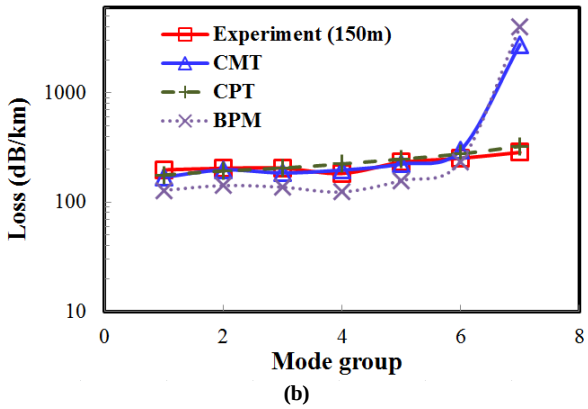


Fig. 3. Loss of (a) a 100m 5-MG RCF and (b) 150m 7-MG RCF obtained from experimental measurement and simulation using CMT/CPT/BPM.

the spatial power spectrum for the 5-MG RCF is much lower than that for the 7-MG RCF in the range $\Delta\beta > (n_{lg}-n_c)k_0$, where $n_{lg}$ is effective index of the last guided mode group. It implies relatively weak (strong) mode coupling for the 5 (7)-MG RCF. As shown in Fig. 2(b), the mode coupling coefficient between neighbouring mode groups calculated with Eq. (6) for the 5-MG RCF is also lower than that for the 7-MG RCF. For the 5 (7)-MG RCF, the decrease (increase) in mode coupling coefficient with increasing mode group index indicates the relatively weak mode coupling in the high (low) mode groups. This is confirmed from the impulse responses of these two 100m 5/7-MG RCFs in Fig. 2 (c) when all the mode groups are excited with equal power. In the figure, for the 5-MG RCF the plateau between the last two pulses (high order mode groups) due to mode coupling is relatively lower than others between the beginning pulses (low order mode groups). For the 7-MG RCF, the impulse response (mode groups) significantly decreases with increasing relative delay (mode group index) because of the strong mode coupling across all the mode groups and the large coupling coefficient in the high order mode groups as mentioned for Figs. 2(a,b). Therefore, only the first several pulses (low order mode groups) were observed, which is consistent with our experimental observation.

With the identified parameters for the relatively weak (strong) mode coupling in the 5 (7)-MG RCF, the bend loss of the RCFs is calculated with the CMT/CPT in Fig. 3. As shown in the figure, the graphs of the bend loss calculated with the CMT for the 5/7-MG RCFs are close to the graphs of the

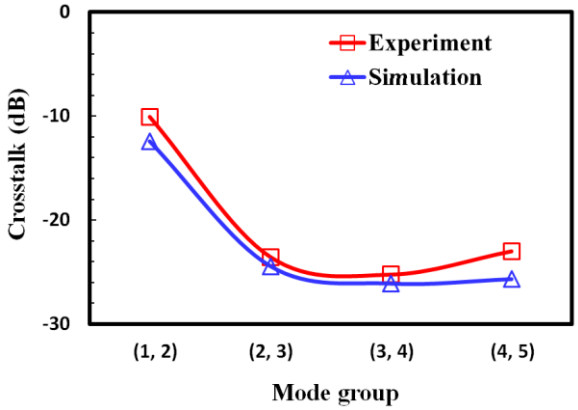


Fig. 4. Crosstalk between neighbouring mode groups for the 100m 5-MG RCF.

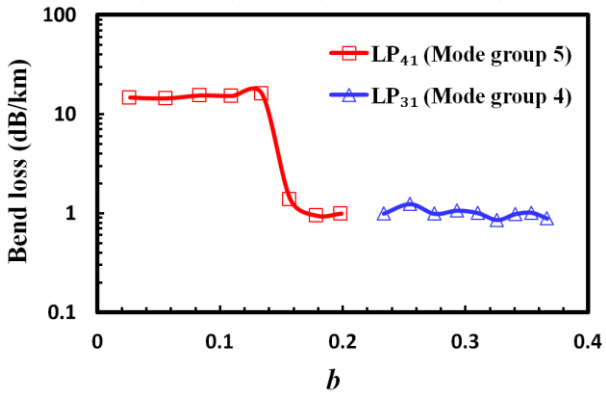


Fig. 5. Bend loss of mode group 5/4 ($LP_{41}$/ $LP_{31}$) for the 5-MG RCF. $\sigma$=35nm, $L_c$=1mm, $p$=2

measured MDL, which shows good agreement in bend loss between simulation and experimental results. To verify the validity of the bend loss calculated with the CMT, the beam propagation method (BPM) is used to obtain bend loss of a ~40mm RCF with microbends [27]. As seen in Fig. 3, the good agreement in bend loss between using the CMT and BPM indicates that the analytical expression in Eq. (2) with the form of the spatial power spectrum in Eq. (3) can be used to accurately predict bend loss of the RCFs. It is interesting to note that, for the 7-MG RCF, the calculated loss of the last guided mode group with the CMT/BPM is higher than the measured loss. This is because the strong mode coupling between the last guided mode group and other guided mode groups or cladding modes in the 7-MG RCF causes the power in the last mode group coupled to the low order mode group. In this case, the measured MDL has a nearly uniform distribution on all the mode groups. As a confirmation, the impulse response of the 7-MG RCF in Fig. 2(c) shows a broad single pulse due to the strong mode coupling. For the 5-MG RCF, the bend loss given by the CPT also agrees well with the measured loss because of the relatively weak mode coupling between different mode groups.

For the interest of low bend loss, the crosstalk for the 100m 5-MG RCF is calculated for the comparison with the experimental result in Fig. 4. It shows that the calculated crosstalk between neighbouring mode groups, which decreases with increasing mode group index, agrees well with the experimental values. The measured crosstalk between mode group (4,5) is slightly higher than mode group (3,4) because the last mode group suffers the highest loss due to microbending as shown in Fig. 3(a). The good agreement between the numerical and experimental results confirms again the validity of the proposed form of the spatial power spectrum with the identified parameters.

### *B. Impact of fibre design on bend loss/crosstalk of the RCFs*

To explore key parameters of the RCFs affecting SDM applications, in this section, the impact of the $\alpha$ and $\Delta$ parameters in the defined refractive index profile in Eq. (9) on bend loss/crosstalk of the RCFs is investigated with the identified parameters for the relatively weak/strong mode coupling in the 5/7-MG RCFs. In the following simulation, the analytical expression with the spatial power spectrum in Eqs. (2-3) and the coupled power equation in Eq. (5) are used to obtain bend loss and crosstalk of the RCFs, respectively.

In practice, the last guided mode group normally suffers the largest bend loss because its smallest $b$ value among the guided mode groups as seen in Fig. 1(b) means that its effective index is close to the cladding index of the RCFs. An effective way of improving bend loss of the RCF is to increase the $b$ of the last mode group by varying ring-core radius of the RCFs. As an example, Fig. 5 shows the bend loss of the last two guided mode groups in a 5-MG RCF, where the parameters $\Delta$=0.01, $\alpha$=2, $d$=5.7$\mu m$ are chosen to mimic the measured RIP in Fig. 1(a). Since the ring-core radius of the RCF affects not only effective index (or $b$) of azimuthal modes, but also the number azimuthal modes, in Fig. 5 the ring-core radius varies from 6.0$\mu m$ to 7.6$\mu m$ to ensure 5 guided mode groups in the RCF. As shown in the figure, for $b$ > 0.15 the bend loss of the last guided mode group ($LP_{41}$) sharply drops to a minimum value, which is nearly equal to the bend loss of the last second mode group ($LP_{31}$). Compared with the experimental result in Fig. 3(a), the loss of the last mode group is significantly improved using the optimized ring-core radius, $r_a$ =7.2~7.6 $\mu m$ ($b$ = 0.15~0.2). To achieve low bend loss of the RCFs, the ring-core radius, $r_a$, and thickness, $d$, are set to ensure that the $b$ of the last guided mode group reaches its maximum value.

After the discussion about the influence of the ring-core radius on the bend loss of the last mode group, the impact of the refractive index contrast $\Delta$ and the gradient parameter $\alpha$ on bend loss of the 5/7-MG RCFs is presented in Fig. 6. As shown in Figs. 6(a,b,e,f) when $\Delta$=0.01, for the $\alpha$ values from 1 to 200, the overall bend loss on the mode groups for either 5-MG or 7-MG RCF remains roughly the same, and the bend loss slightly increases with increasing mode group index. This indicates that the gradient parameter $\alpha$ has a little influence on bend loss of the RCFs with weak/strong mode coupling. For $\alpha$=200, the RCFs can be considered to have a step-index profile.

Figs. 6 (c,d,g,h) show bend loss of the 5/7-MG RCFs for the $\Delta$ values of 0.005, 0.01, 0.02 when $\alpha$=2. The RCFs with a larger

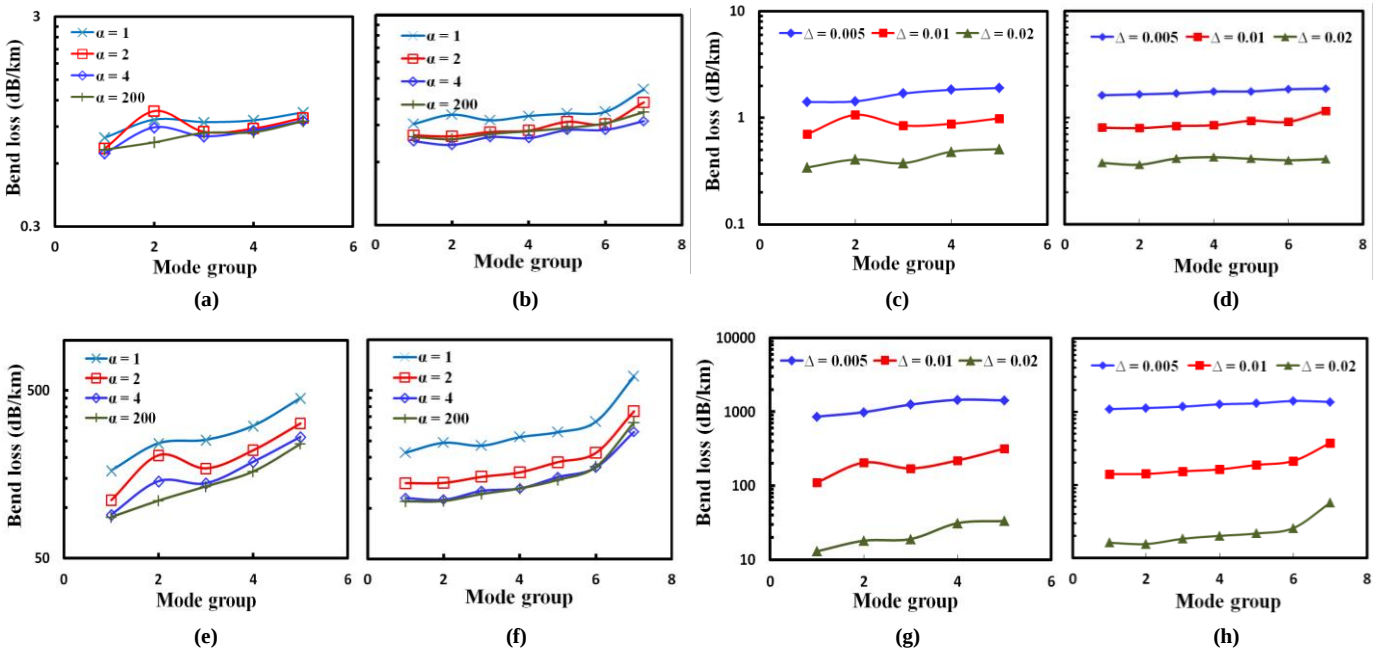


Fig. 6. Bend loss of the 5/7-MG RCFs for different values of (a,b,e,f) $\alpha$ ($\Delta$ =0.01) or (c, d, g, h) $\Delta$ ($\alpha$=2). $\sigma$=35nm (a-d): $L_c$=1mm, $p$=2; (e-h): $L_c$=0.083mm, $p$=3.

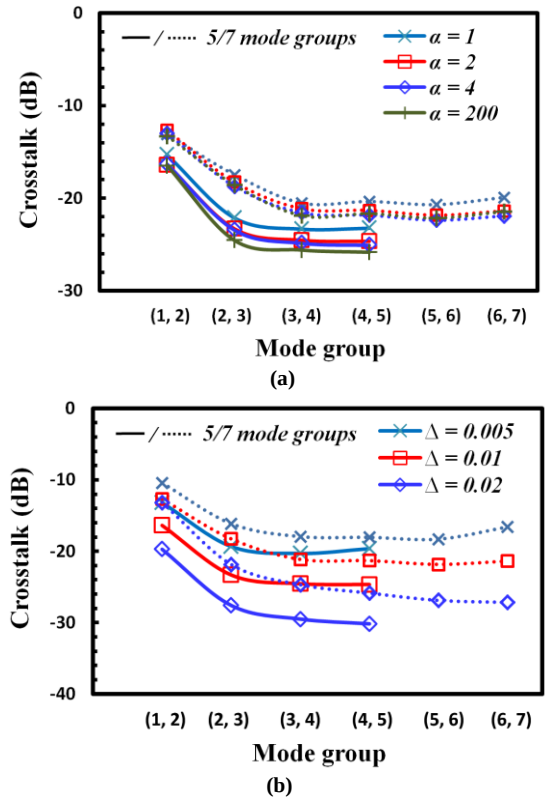


Fig. 7. Crosstalk between neighbouring mode groups in the 1km 5/7-MG RCFs for different values of (a) $\alpha$ ($\Delta$ =0.01) and (b) $\Delta$ ($\alpha$=2). $\sigma$=35nm, $L_c$=1mm, $p$=2.

$\Delta$ have the smallest bend loss. With the parameters for weak (strong) mode coupling, the bend loss for the RCFs is improved by two (ten) times when the $\Delta$ value is doubled. Such big improvement in bend loss by a large $\Delta$ is due to increased $\Delta\beta$ between neighbouring mode groups. The same magnitude improvement in bend loss for both the 5/7-MG RCFs indicates that the bend loss improvement by increasing the $\Delta$ is dependent on the spatial power spectrum instead of the number of guided mode groups in the RCFs.

With the calculated bend loss of mode groups in Fig. 6, the crosstalk between neighbouring mode groups in the 1km 5/7-MG RCFs for different $\alpha$ or $\Delta$, is obtained in Figs. 7(a,b) where the parameters for weak mode coupling are used. As shown in the figures, the crosstalk for the 5/7-MG RCFs decreases with increasing mode group index, and the 5-MG RCFs always have a crosstalk lower than the 7-MG RCFs for the same $\alpha$ and $\Delta$ values. In Fig. 7(a) where $\Delta$=0.01, for the 5/7-MG RCFs, the graphs of the crosstalk for different $\alpha$ are close to each other, which means that the $\alpha$ does not significantly affect the crosstalk. However, Fig. 7(b) shows a significant improvement in crosstalk by increasing the $\Delta$ for the 5/7-MG RCFs. The crosstalk in the high order mode groups is improved more than that in the low order mode groups.

## V. Conclusions

Numerical and experimental investigations of the mode coupling in the 5/7-MG RCF have been undertaken with the coupled mode/power theory and a proposed form of spatial power spectrum. Simulations have shown a good agreement in bend loss and crosstalk between numerical and experimental results based on the identified parameters for the spatial power spectrum in the 5/7-MG RCF. Impact of the $\alpha$ and $\Delta$ parameters of the RCF on bend loss and crosstalk have also been investigated, which shows that the $\Delta$ instead of the $\alpha$ significantly affects bend loss and crosstalk of the RCF. The magnitude improvement in bend loss by increasing the $\Delta$ is dependent on the spatial power spectrum of random perturbations of fibre axis rather than the number of guided

mode groups in the RCF.

## References


[1] H.R. Stuart,"Dispersive Multiplexing in Multimode Optical Fiber," Science, vol. 289, no. 5477, pp. 281-283, Jul. 2000.

[2] D.J. Richardson, J. M. Fini, and L. E. Nelson, "Space-division multiplexing in optical fibres," Nat. Photonics, vol. 7, pp. 354–362, May 2013

[3] P.J. Winzer, 'Scaling optical fiber networks: challenges and solutions,' Optics & Photon. News, Mar. 2015

[4] R. Ryf, S. Randel, A. H. Gnauck, C. Bolle, A. Sierra, S. Mumtaz, M. Esmaeelpour, E. C. Burrows, R.-J. Essiambre, P.J. Winzer, D.W. Peckham, A. H. McCurdy, and R. Lingle, "Mode-Division Multiplexing Over 96 km of Few-Mode Fiber Using Coherent 6 × 6 MIMO Processing", J. Lightwave Technol., vol. 30, no.4, pp. 521–531, Feb. 2012.

[5] Y. Chen, A. Lobato, Y. Jung, H. Chen, V.A.J.M. Sleiffer, M. Kuschnerov, N.K. Fontaine, R. Ryf, D.J. Richardson, B. Lankl, and N. Hanik, "41.6 Tb/s C-band SDM OFDM Transmission through 12 Spatial and Polarization Modes over 74.17 km Few Mode Fiber," J. Lightwave Technol., vol. 33, no. 7, pp. 1440–1444, Apr. 2015

[6] B.C. Thomsen, "MIMO enabled 40 Gb/s transmission using mode division multiplexing in multimode fiber", Optical Fiber Communication/National Fiber Optic Engineers Conference (OFC/NFOEC), (USA, 2010), Paper OThM6

[7] M. Yoshida, S. Beppu, K. Kasai, T. Hirooka and M. Nakazawa, "1024 QAM, 7-core (60 Gbit/s x 7) fiber transmission over 55 km with an aggregate potential spectral efficiency of 109 bit/s/Hz," J. Lightwave Technol., vol. 23, no. 16, pp. 20760–20766, Jul. 2015

[8] S. Jain, V.J.F. Rancaño, T.C. May-Smith, P. Petropoulos, J.K. Sahu, and D.J. Richardson, "Multi-Element Fiber Technology for Space-Division Multiplexing Applications," Opt. Express, vol. 22, no. 4, pp. 3787–3796, Feb. 2014.

[9] N. Bozinovic, Y. Yue, Y. Ren, M. Tur, P. Kristensen, H. Huang, A.E. Willner, and S. Ramachandran, "Terabit-Scale Orbital Angular Momentum Mode Division Multiplexing in Fibers", Science, vol. 340, no. 6140, pp. 1545-1548, Jun. 2013.

[10] C.R. Doerr, N.K. Fontaine, M. Hirano, T. Sasaki, L.L. Buhl, and P.J. Winzer, "Silicon photonic integrated circuit for coupling to a ring-core multimode fiber for space-division multiplexing", European Conference and Exhibition on Optical Communication (ECOC 2011), Paper Th.13.A.3

[11] M. Hirano, Y. Yamamoto, Y. Tamura, T.Haruna and T. Sasaki, "Aeff-enlarged Pure-Silica-Core Fiber having Ring-Core Profile", Optical Fiber Communication/National Fiber Optic Engineers Conference (OFC/NFOEC), (USA, 2012), Paper OTh4I.2

[12] X.Q. Jin, R. Li, D.C. O'Brien, and F.P. Payne, "Linearly Polarized Mode Division Multiplexed Transmission over Ring-Index Multimode Fibres", IEEE Summer Topicals, (USA, 2013), pp. 113-114.

[13] Q. Kang, E. Lim, Y. Jun, X.Q. Jin, F.P. Payne, S. Alam, and D.J. Richardson, "Gain Equalization of a Six-Mode-Group Ring Core Multimode EDFA", European Conference and Exhibition on Optical Communication (ECOC 2014), Paper P.1.14

[14] N.K. Fontaine, R. Ryf, M. Hirano, T. Sasaki, "Experimental Investigation of Crosstalk Accumulation in a Ring-Core Fiber", IEEE Summer Topicals, (USA, 2013), Paper TuC4.2

[15] C. Brunet, B. Ung, P.-A. Belanger, Y. Messaddeq, S. LaRochelle, and L.A. Rusch, "Vector Mode Analysis of Ring-Core Fibers: Design Tools for Spatial Division Multiplexing," J. Lightwave Technol., vol. 32, no. 23, pp. 4648–4659, 2014.

[16] C. Brunet, P. Vaity, Y. Messaddeq, S. LaRochelle, and L.A.Rusch, "Design, fabrication and validation of an OAM fiber supporting 36 states," Opt. Express, vol. 22, no. 21, pp. 26117–26127, Oct. 2014.

[17] M. Kasahara, K. Saitoh, T. Sakamoto, N. Hanzawa, T. Matsui, K. Tsujikawa, and F. Yamamoto, "Design of Three-Spatial-Mode Ring-Core Fiber," J. Lightwave Technol., vol. 32, no. 7, pp. 1337–1343, Apr. 2014.

[18] B. Ung, P. Vaity, L. Wang, Y. Messaddeq, L.A. Rusch, and S. LaRochelle, "Few-mode fiber with inverse-parabolic graded-index profile for transmission of OAM-carrying modes," Opt. Express, vol. 22, no. 15, pp. 18044–18055, Jul. 2014.

[19] X.Q. Jin, A. Gomez, D.C. O'Brien, and F.P. Payne, "Influence of Refractive index profile of ring-core fibres for space division multiplexing systems", IEEE Summer Topicals, (USA, 2014), pp.178-179, Jul. 2014

[20] F. Feng, G. S. D. Gordon, X. Q. Jin, D. C. O'Brien, F. P. Payne, Y. Jung, Q. Kang, J. K. Sahu, S. U. Alam, D. J. Richardson, and T. D. Wilkinson, "Experimental characterization of a graded-index ring-core fiber supporting 7 LP mode groups," OFC/NFOEC'2015, Paper Tu2D.3, Mar. 2015

[21] F. Feng, X. Guo, G. S. D. Gordon, X. Q. Jin, F. P. Payne, Y. Jung, Q. Kang, S. Alam, P. Barua, J. K. Sahu, D. J. Richardson, I.H. White and T. D. Wilkinson, "All-optical Mode-Group Division Multiplexing Over a Graded-Index Ring-Core Fiber with Single Radial Mode," OFC/NFOEC'2016, submitted.

[22] D. Marcuse, "Microbending Losses of Single-Mode, Step-Index and Multimode, Parabolic-Index fibers," Bell Syst. Tech. J., vol. 55, no. 7, pp. 937–955, Sep. 1976.

[23] D. Marcuse, "Microdeformation losses of single-mode fibers.," Appl. Opt., vol. 23, no. 7, pp. 1082-1091, Apr. 1984.

[24] R. Olshansky, "Mode Coupling Effects in Graded-index Optical Fibers", Applied Optics, vol. 14, no. 4, pp. 935-945, April 1975

[25] D. Marcuse, "Derivation of coupled power equations", Bell Syst. Tech. J., vol. 51, no. 1, pp. 229-237, January 1972

[26] D. Yevick and B.Stoltz, "Effect of mode coupling on the total pulse response of perturbed optical fibers", Applied Optics, vol. 22, no. 7, pp. 1010-1015, April1983

[27] X.Q. Jin and F.P. Payne, "Numerical investigation of microbending loss in optical fibres", J. Lightwave Technol., submitted

[28] K. Shi, A. Gomez, X.Q. Jin, Y. Jung, C. Quintana, D.C. O'Brien, F.P. Payne, P. Barua, J. Sahu, Q. Kang, S-U Alam, D.J. Richardson and B.C. Thomsen, "Simplified Impulse Response Characterization for Mode Division Multiplexed Systems," OFC/NFOEC'2016, submitted.